Structural Analysis of Historical Constructions – Anamnesis, diagnosis, therapy, controls – Van Balen & Verstrynge (Eds)
 ISBN 978-1-138-02951-4

Assessing the physical-mechanical properties of ferruginous sandstone

R. Hayen, L. Fontaine & H. De Clercq
Royal Institute for Cultural Heritage, Brussels, Belgium

ABSTRACT: A dark-brown glauconite-rich sand cemented by iron oxides characterizes the landscape and the typical architecture of the Hageland: the so-called ferruginous sandstone of the Diest Formation.

This paper describes the results of a material-technical research of this ferruginous sandstone, excavated from sedimentary beds at five locations, with the aim to evaluate their potential use for restoration purposes. The correlation of the physical-mechanical properties of the ferruginous sandstone with either ultrasound or petrographic characterization was evaluated as part of a quality assessment of the material.

Although the evaluation of the ultrasound wave velocity proved useful for the selection of the samples, the statistical analysis evidenced only a general correlation with the different physical-mechanical properties. The petrographic analysis, on the other hand, could effectively address the lithification properties of the ferruginous sandstone, which could be positively related to the density, the porosity and the strength characteristics of the material.

1 INTRODUCTION

The ferruginous sandstone of the Diest Formation is a dark-brown building stone typical for the late gothic architecture of the Hageland, the eastern part of the Belgian province Flemish Brabant. The spreading of this ferruginous sandstone is determined by the hills of the Hageland and extends to the southern Campine and the Brabant loamy region (Dusar et al. 2009), agreeing more or less with the area where this material has dominantly been used for construction works.

2 GEOLOGICAL HISTORY

The Diest Formation is a glauconite-rich siliceous sand unit with a maximum thickness of about 100 m. In the Hageland it is of late Miocene age where it unconformably overlies the older Cenozoic strata. Filling a strongly incised valley, which was submerged due to sea-level rise ca. 10 million years ago (Vandenberghe et al. 2014), the sandbanks were deposited in a shallow marine environment. From as early as the Pliocene, the uplift in the Ardennes-Eifel region caused the sands of the Diest Formation to emerge from the marine environment.

Processes related to soil formation might explain why the sands turned into sandstone (lithification). Glauconite (an iron-rich phyllosilicate made up of agglomerated clay particles) decomposed into individual clay particles and iron-(hydr)oxides. These compounds were transported by percolating waters to the groundwater table, where the water movement is very low, enabling the chemical precipitation of the iron-(hydr)oxides in the pore space around the sand grains. The accumulated iron-(hydr)oxides act as a cement between the sand grains (Dusar & De Ceukelaire 2014). Depending on the quantity, the composition and the crystallinity of the cement various degrees of internal cohesion can be observed in the ferruginous sandstone of the Diest Formation.

3 ARCHITECTURAL HISTORY OF THE FERRUGINOUS SANDSTONE AS A BUILDING MATERIAL

The hilly landscape of the Hageland is characterized by a sequence of south to south-east oriented ridges. In Roman times the flanks of these hills were used to cultivate wine. A tradition which has recognized a successful revival in recent years. The geologic origin of these hills therefore not only influenced the regional culture and history, but is reflected as well within the local architecture as the hilltops are characterized by the presence of layers of ferruginous sandstone (Bos & Gullentops 1990, Doperé et al. 2003).

The use of ferruginous sandstone as a construction material reaches back to the Roman era. Between 1979 and 1983, the remains of a cellar from a Roman villa from the 2nd century AD were excavated at the 'Stenen Kruis' in the municipality of Bierbeek. The cellar walls were constructed entirely in finely dressed ferruginous sandstone masonry, most probably originating from the Brussels or Tongeren Formation (Deweerdt 1980, Deweerdt & Provoost 1982, Bos & Gullentops 1990, Dusar et al. 2009). A few decades later another Roman villa in Rotselaar was excavated, of which the foundations were constructed with a locally quarried ferruginous sandstone (Middelbergpark 2009).

During the Gallo-Roman period, the use of brick and stone masonry for construction purposes declined only to revive by the 10th century. The earliest examples of the re-use of ferruginous sandstone as a construction material date from the 11th century. Today, only two examples remain of these early Romanesque churches where the tower was constructed entirely with ferruginous sandstone: the St. Catherine's Church of Kortrijk-Dutsel and the Church of Our Lady's Birth of Oostham. Until recently also the St. Willibrord's Church of Meldert was a fine witness of this early Romanesque period. However, its tower collapsed on the 7th of July 2006. All these early Romanesque towers were constructed with ferruginous floats, rather thin (between 2 and 3 cm thick) brown-black limonite concretions which could easily be found on the hilltops of the Hageland. Also the tower of the St. Martin's Church of Beek, near Bree, was mainly constructed with such floats.

Constructions with larger, more or less finely dressed ferruginous sandstone blocks appeared only as early as the 12th century, since the excavation of such stone blocks required the exploitation of ferruginous sandstone layers at a relatively important depth. In the beginning the masonry structures were conceived as a multiple leaf wall with the outer façades built with finely dressed sandstone blocks and the internal part consisting of a mixture of ferruginous floats and lime mortar (Callebaut 1982). Later on, the internal part consisted at times of regular brick masonry. The tradition of using the ferruginous sandstone for interior and exterior facing gradually developed into a characteristic local architecture, characterized by columns and semi-columns free of capitals, broad niches in the walls of the choir's apse and alternating layers of ferruginous sandstone and light-coloured sandy limestone, mostly from the Lede or the Brussels Formation (Figure 1). The difficulty of sculpting the ferruginous sandstone is most probably responsible for the lack of finely detailed ornaments within such architecture (Doperé et al. 2003). The use of the ferruginous sandstone remains at that time prominent, as the imported limestones were far more expensive. About 30 churches remain from this period.

In the late Medieval period, the use of ferruginous sandstone is no longer limited to religious architecture, but gradually becomes quite current for civil constructions such as castles, donjons, town walls and gates, cloth halls, farms, etc., although often combined with brick and limestone and its use even regularly remaining restricted to foundations and plinth areas.

As from around 1500, the use of ferruginous sandstone declines both in religious and profane architecture. For the construction of the late Gothic churches the more prestigious lightly colored sandy limestones are preferred. Wherever ferruginous sandstone is applied, mainly in the interior, the masonry is finished with a plaster within the habit of the period. For civil constructions, on the other hand, straight brickwork masonry is preferred except for utility constructions exposed to running water (e.g. watermills, sluices, quaysides and bridge pillars). For some unknown reasons, ferruginous sandstone remains preferred for constructions in contact with running water, and this until it is replaced by the compact bluestone of Tournai by the early 19th century.

Figure 1. Typical example of the local architecture found along the Demer river: Our Lady's Church of Aarschot. Ferruginous sandstone is alternated with layers of the light-coloured sandy limestone of Gobertange (Brussels Formation).

By then, most commercial exploitation of ferruginous sandstone of the Diest Formation apparently no longer exists, with the exception of some local, temporary excavations. All of this changes towards the end of the 19th century following the need for replacing severely weathered stone blocks of several monuments, amongst others, the Our Lady's Church of Aarschot, the Maiden Tower of Zichem and the St. Sulpice's and St. John's churches of Diest. Some quarries re-open, like the 'Wijngaardberg' at Wezemaal and the 'Steenkot' at Kelbergen (RLNH 2007).

Ferruginous sandstone is well known as a heterogeneous construction material, sensitive to erosion and often leading to a very heterogeneous damage pattern, which makes the selection of suitable materials and intervention techniques for restoration difficult (Figure 2). Some stone blocks may exhibit at first sight practically no damage, while neighboring blocks may have lost their internal cohesion and exhibit material loss over several centimeters depth. Such variations can appear even within a single block of ferruginous

Figure 2. A typical example of damage to the ferruginous sandstone at the St. Catherine's Church of Kortrijk-Dutsel.

Table 1. Literature values for the compressive strength of ferruginous sandstone from monuments and quarries.

Location	#	f_c N/mm^2
St. Eustache's church, Zichem (Triconsult 2007)	19	2.5
Maiden tower, Zichem (Van Campenhout 2009)	15	6–17
Middelberg, Rotselaar (Van Campenhout 2009)	4	5–15
Weefberg, Averbode (Van Campenhout 2009)	24	10–23
St. Willibrord's church, Meldert (Bourel, 2010)	10	7.2 ± 5.3
Kepkensberg, Tessenderlo (Dreesen et al. 2010)	9	17.0 ± 4.4
Roeselberg, Herent (De Schutter & De Pau, 2010)	10	6.4 ± 2.6
Maiden tower, Zichem (Hayen & De Clercq 2011)	10	5.9 ± 1.5

sandstone, where softer zones may have disappeared to quite an extend while more solid limonite layers or concretions still outline the original surface of the stone. The cause of damage can be very diverse, being related for instance to the effect of frost, salts or wind erosion. Nevertheless it always comes down to the loss of cohesion of the stone opposed to the initial degree of lithification of the sand. In general, it is considered a rather weak building material, especially in comparison with other typical local building materials such as Gobertange, Lede or Tournai stones. Typical values for the compressive strength (f_c) found in the literature are reported in Table 1.

4 STONE MATERIAL

The petrographic and physical characterization of the ferruginous sandstone from the Diest Formation is based on core drillings lifted at 5 sites: Roeselberg (Herent), Gasthuisbos (Pellenberg), Beninksberg (Wezemaal), Middelberg (Rotselaar) and Langenberg (Diest). At the first four sites, stone layers as deep as 21 meters depth were drilled (Table 2). At Langenberg a total of 15 surficial cores were lifted for the study through drilling up to a depth of 1.2 m straight from the stone layers, of which the upper surface corresponds to the slope hill. In the future parts of the slope hill will be cut away to straighten the road curve, leaving a resource of potential restoration material.

Table 2. Description of the location of the core drillings.

Site	Geographic coordinates Longitude	Latitude	Depth m
Beninksberg	50°56′46.22″N	4°47′10.58″E	13.0
	50°56′45.78″N	4°47′08.39″E	12.15
	50°56′45.87″N	4°47′07.89″E	11.00
Gasthuisbos	50°53′03.34″N	4°46′32.36″E	16.00
	50°53′05.04″N	4°46′33.90″E	20.50
Langenberg[1]	50°59′40.66″N	5°01′53.63″E	<1.20
Middelberg	50°57′45.96″N	4°46′16.13″E	20.50
	50°57′44.45″N	4°46′16.78″E	10.15
Roeselberg	50°53′46.63″N	4°41’02.93″E	21.65

[1]Averaged position of the 15 drillings.

The core drillings were visually classified from compact (class I) to crumbly material (class III). The quality was empirically assessed on-site by means of gently hammering of the stone. This quality assessment aimed to describe the successive stone layers and was the initial sampling criterion for further characterization of the ferruginous sandstone material.

5 METHODOLOGY

5.1 *Ultrasound propagation velocity*

The non-destructive method to determine the ultrasound propagation velocity was chosen with the objective to select samples for further analysis and hence to set up a research program. The core drillings (approximately 10 cm in diameter) were left to dry for at least 3 weeks at 20°C and 60% relative humidity (RH). After that, the velocity of ultrasound waves was measured in two orthogonal directions across the cylindrical cores at each centimeter along its length (in total almost 4000 measurements were realized). As such, ultrasound wave velocity profiles were obtained along the length of the core drillings, enabling a statistical analysis of the ultrasound wave velocity of ferruginous sandstone and a correlation with the earlier defined on-site quality assessment.

5.2 *Compressive strength*

The compressive strength was determined according to the standard EN 1926:2006 'Natural stone test methods. Determination of uniaxial compressive strength'. The tests are realized on a total of 37 cubic samples with edges of 50 ± 5 mm (23 samples) or 70 ± 5 mm (14 samples), though one of the small sample exceeded the given tolerances in the height.

The samples were dried prior to the test at 70 ± 5°C till a constant weight was achieved. The samples were consequently tested perpendicular to the bedding at a constant compression rate of 0.34 N/mm^{2}s.

5.3 *Frost resistance*

The frost resistance was determined according to the standard EN 12371:2010 'Natural stone test methods. Determination of frost resistance'. The tests are realized on a total of 18 beams with varying dimensions, according to maximum obtainable size from the given stone blocks. The size of the smallest face of the beam varied between 5 to 8 cm by 6 to 7 cm, whereas the height of the beams varied between 9 to 30 cm.

According to the standard a sample is considered 'broken' if at least one of the following conditions is met: i) when one of the following phenomena are observed through visual inspection: cracks having a width of at least 0.1 mm, the appearance of holes or the detachment of fragments more than 30 mm^2 in size, ii) the loss of the dynamic elastic modulus is equal or larger than 30% or iii) the decrease of the apparent volume is larger than 1%. In practice, the last criterion is no longer in use as it is subordinate to the first two criteria. In the particular case of ferruginous sandstone, the first criterion is less evident as the heterogeneous samples often initially already present such irregularities making it difficult to assess additional damage. Hence, in practice the loss of the dynamic elastic modulus, characteristic for the fracturing and ultimate disintegration of the sample, was considered as the main criterion for determining the frost resistance of ferruginous sandstone.

6 PETROGRAPHIC AND PHYSICAL CHARACTERIZATION OF THE FERRUGINOUS SANDSTONE FROM THE DIEST FORMATION

6.1 *Velocity of ultrasound waves*

An established laboratory method to assess the quality of rock consists of the measurement of the propagation of ultrasound waves. Yet the application of this technique on very heterogeneous rocks, such as ferruginous sandstone, is less evident, even more the possibility to extend its application to on-site conditions as the propagation velocity of sound waves through a porous solid is further influenced by a number of external factors, in particular the moisture content.

After a first visual selection of the drilled cores, described in point 4, individual fragments were submitted to ultrasound wave propagation tests as a contribution for the quality assessment. The ultrasound wave velocity of ferruginous sandstone varies from ca. 400 m/s for a loosely coherent sand up to more than 3500 m/s for compact sandstone. The error margin on individual measurements is estimated at 17.5 m/s, which is considerably smaller than the natural variation of the velocity as a consequence of heterogeneity and bedding orientation of the sandstone. It was even possible to assign the bedding of the rock, even if visually unrecognizable, as the direction perpendicular to the stratification is characterized by a significant lower propagation velocity (ca. 30% difference).

The comparison of the ultrasound wave velocity with the on-site empirical quality assessment evidences a general correlation between both. However, considerable overlap is observed amongst the quality classes. Fragments also often showed a strong variation of ultrasound wave velocity along their length, whereas their quality was assessed by a single classification.

6.2 *Petrographic characterization*

The ferruginous sandstone from the Diest Formation is a dark-brown natural stone formed through the cementation of a glauconite-rich siliceous sand by a ferruginous binder (De Clercq & Dusar 2011, De Clercq et al. 2009, De Clercq et al. 2010a, b, De Clercq et al. 2012). Not weathered glauconite grains can give the stone a green hue. Within the ferruginous sandstone iron concretions can occur as limonite layers or rings. Bioturbations caused by the activity of marine burrowing organisms at the time of deposition are also regularly found.

The petrographic analysis of thin-sections revealed the existence of different forms of the cement. Based on its appearance under normal (non-polarized) light two types of cement can be recognized: a dark (almost opaque) and a light cement (more or less transparent or translucent).

The dark cement, here arbitrarily described as the limonite cement, is definitely the most recurrent form of binding medium. It can take various forms: i) microcrystalline aggregates (Figure 3), ii) crystallites, iii) thin (single layered) to thick (multiple layered) crusts up to iv) a continuous and dense binder matrix (Figure 4). The term limonite describing the cement is arbitrarily as limonite itself is already a vague notification referring to a mixture of iron oxides and iron hydroxides without giving detailed information on the purity, the exact chemical or mineralogical composition, the crystallinity nor the possible clay content. The very nature of the light cement (Figure 5) has so far not been exactly identified, but it is presumably rich in clay minerals.

The characteristics of the binding medium were semi-quantitatively addressed by means of petrographic analysis, enabling a classification of the ferruginous sandstone into three categories according to their degree of lithification: weak, moderate and strong. A strong lithification of the ferruginous sandstone is the result of a continuous and dense deposit

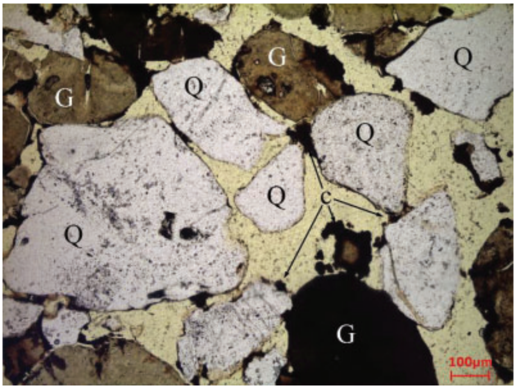

Figure 3. Petrographic micrograph of a weakly lithified sandstone of the Diest Formation from Roeselberg (Herent). The dark limonite cement (c) appears as isolated islands at the contact points between sand grains (Q = quartz, G = glauconite).

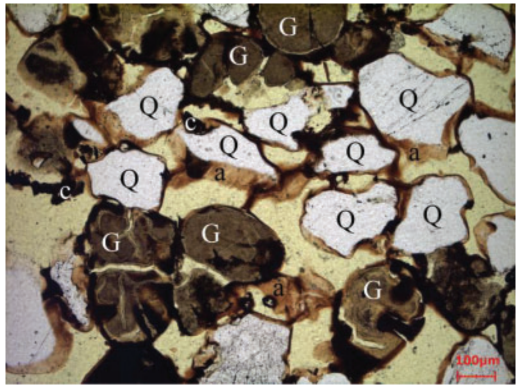

Figure 5. Petrographic micrograph of a weakly lithified sandstone from the Diest Formation from Beninksberg (Wezemaal). The sand grains (Q = quartz, G = glauconite) are covered with a light more or less transparent microstalactitic cement (a). Locally isolated dark-colored microcrystalline limonite aggregates (c) can be recognized.

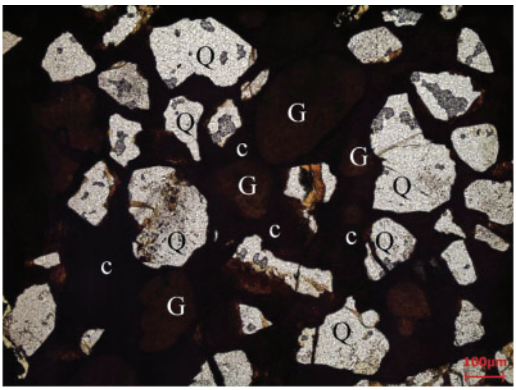

Figure 4. Petrographic micrograph of a strongly lithified sandstone from the Diest Formation from Langenberg (Diest). The dark limonite cement (c) densely fills the entire pore space between the sand grains (Q = quartz, G = glauconite).

of the limonite cement around sand grains and a general high amount of cement (from 10 to more than 20%), whereas weakly lithified ferruginous sandstone is characterized by a low amount of binding medium (generally below 5% up to maximum 10%) consisting of individual islands of limonite between neighboring sand grains. Moderately lithified ferruginous sandstone falls somewhere in between with a discontinuous deposit of the limonite of which the amount ranges from 5 to 15%. As the amount of limonite and degree of filling of the pore volume increases with lithification, the total macro-porosity (pores larger than ca. 100 μm in diameter), the average pore size and their connectivity decrease consequently.

The comparison of the petrographic observations and the on-site empirical quality assessment evidences that such an on-site evaluation is a reasonable indication for the degree of lithification of the ferruginous sandstone. However, the on-site determination is not an entirely closely-reasoned prove as it is often an assessment for a fragment as a whole, which might show important variations in degree of lithification as a result of the inherent heterogeneity of the ferruginous sandstone. The same conclusion applies for the comparison of the ultrasound propagation velocity and the degree of lithification.

6.3 *Compressive strength*

Defects, such as voids, cracks or broken corners, were noticed on several samples which normally lead to their rejection for compressive testing. However, as such defects are quite typical for the material applied for construction purposes, they were as such included in the program. Hence, as expected, a broad variety of results in compressive strengths was obtained, varying between 2.1 and 37.2 N/mm^2 with an average value of 14.0 ± 9.9 N/mm^2. Values which are, except for the best quality of stones, in agreement with those available in the literature (Table 1).

When comparing the material properties, a rather weak correlation is observed between the density and the compressive strength of ferruginous sandstone. Such a weak correlation comes as no surprise as the ferruginous sandstone is known for its heterogeneity, including limonite concretions and voids which strongly influence the crack development and hence compressive strength of the samples. Based on the data the following formula can be applied to determine a minimal compressive strength from the density of the stone:

$$f_c\ (N/mm^2) = 0.004\ e^{0.0035\ \rho_b\ (kg/m^3)} \qquad (1)$$

where f_c = compressive strength; ρ_b = density.

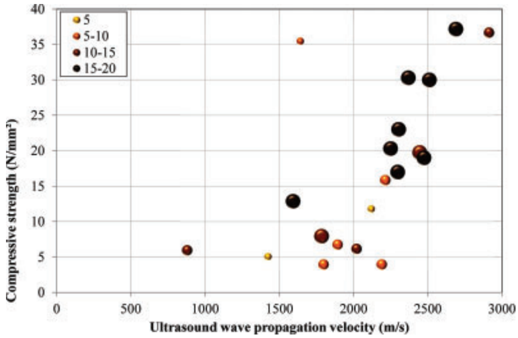

Figure 6. Comparison of the average ultrasound wave propagation velocity (m/s), the compressive strength (N/mm^2) and the characteristics of the limonite cement (the colour refers to the amount of limonite cement, while the size to its distribution properties with small = isolated islands of limonite cement, medium = discontinuous repartition of the limonite cement and large = continuous limonite cement).

However, such an approach seriously underestimates the true strength of most of the ferruginous sandstones, potentially rejecting a lot of good quality material.

When comparing the mechanical strength of ferruginous sandstone with the degree of lithification based on the amount and distribution of the limonite cement, determined from petrographic analysis, a positive correlation is noticed (Figure 6). A strong lithification, characterized by a dense continuous deposit of limonite, corresponds with a compressive strength of at least 15 N/mm^2.

Only one sample doesn't compel to this correlation. Although it concerns a strongly lithified ferruginous sandstone, characterized by a high amount of limonite cement (15–20%) and a continuous deposit surrounding the sand grains, its compressive strength (13 N/mm^2) is lower than expected. This is also the case for the propagation velocity of ultrasound waves. Detailed petrographic analysis of the material evidences however the presence of numerous micro-cracks within the sandstone, which might explain the lower compressive strength. The micro-cracks are presumably the result of frost damage, probably induced at the end of the Last Glacial Maximum when the top layers of the ferruginous sandstone banks, from where the sample was lifted, were exposed to recurring sequences of freeze-thaw cycles.

Despite low amounts of limonite cement and discontinuous deposits, some samples exhibit high compressive strengths. This is especially the case for one sample from the Beninksberg in Wezemaal with an average ultrasound propagation velocity of 1642 m/s and a compressive strength of 35.5 N/mm^2. It is likely that the core of the sample – tested for its compressive strength – exhibited somewhat better characteristics as compared to its edges, where the sample for the petrographic analysis was taken.

Table 3. Overview of the number of samples of ferruginous sandstone which withstood the prescribed number of freeze-thaw cycles (prior to the loss of the dynamic elastic modulus exceeded 30% of the initial value) as function of their degree of lithification. A score of 0 freeze-thaw cycles indicates that the sample failed before 14 cycles were completed.

Degree of lithification	Number of freeze-thaw cycles completed				
		14	56	70	140
weak	1	1	0	0	3
moderate	1	1	1	0	2
strong	1	0	2	0	5

6.4 *Frost resistance*

In total 18 samples were subjected to cyclic freeze-thaw testing. The overview of the number of samples of ferruginous sandstone which withstood the prescribed number of freeze-thaw cycles as function of their degree of lithification is given in Table 3.

The results evidence no correlation at all between the degree of lithification of the ferruginous sandstone and its frost resistance. Although a slight majority of the samples of either weak, moderate and strong lithification have proven to be highly frost resistant, each category contained also frost sensitive material. A preliminary analysis of the pore structure characteristics of a selected number of samples subjected to the freeze-thaw cycles indicates that available literature values to theoretically assess the frost resistance of natural stones based on their pore structure (Ingham 2008) are not directly applicable to ferruginous sandstone. Hence, a reasonable frost resistance may be expected from the ferruginous sandstone, although a criterion to assess the frost resistance from petrographic analysis still remains elusive.

7 CONCLUSION

For restoration purposes, emphasis is often laid upon the compressive strength of the materials concerned. However, when replacing a stone in a façade, the new stone will hardly be loaded afterwards unless additional settlements occur within the built structure. Not so much its mechanical strength, but rather its physical properties are then of concern for the new stone to blend in with the existing material fabric. However, the selection of the materials for this research evidenced that low strength ferruginous sandstone (<5 N/mm^2 compressive strength) is very soft and often easily scratched, leaving opportunities for mechanical erosion (wind and rain erosion, mechanical wear due to vandalism or bicycles, etc.). The use of such soft sandstone is therefore not advised in an outdoor environment.

As for true structural repairs to massive structures, average loads are typically situated in the order of 1 or 2 N/mm^2. Even when considering safety margins to include i) the effect of increased stress concentrations around door and window openings or stairways piercing through the structure, ii) the load redistribution in multiple leaf walls, concentrating the loads on the inner and outer leafs, iii) the effect of creep reducing the material strength over time and iv) the influence of moisture on the strength of ferruginous sandstone in particular (Bourel 2010) a compressive strength of 15 N/mm^2 seems sufficient in most cases. For such structural repairs, a knowledge of the geological context and a petrographic study suffice to guarantee that the minimal mechanical strength criteria are met with a minimum of material required.

However, the structural repair of slender structures such as columns, vault ribs or flying buttresses requires an individual assessment of their structural safety. Yet, for the repair of load-bearing elements requiring higher compressive strengths, ferruginous sandstone with a compressive strength of 30 to 35 N/mm^2 can be found. In such cases an individual compressive strength assessment based on core drillings and experimental research is needed.

Freeze-thaw tests evidence that a reasonable frost resistance may be expected from the ferruginous sandstone, but it should not be considered a general characteristic. Further research is needed to define a simple criterion to assess the frost resistance of ferruginous sandstone.

REFERENCES

Bos, K. & Gullentops, F. 1990. IJzerzandsteen als bouwsteen in en rond het Hageland (in Dutch). *Bulletin de la Société belge de Géologie – Bulletin van de Belgische Vereniging voor Geologie* 99–2, 131–151.

Bourel, E. 2010. Numerieke modellering van tijdsafhankelijk gedrag en faling van monumentale metselwerkstructuren (in Dutch). *Master thesis Civil Engeneering Departement*, K.U. Leuven.

Callebaut, D. 1982. De tafelrondmote op de warande te Diest (in Dutch). *Archaeologica Belgica* 250, Varia IV, 6–18.

De Clercq, H., Hayen, R., Dusar, M., Cnudde, V. & Vanderauwera, M., 2009. Zichem, Maagdentoren, Materiaal-technische studie van de buitenschil (in Dutch). *WTA-conference "Interventies en hun consequenties", Drongen, 13 november 2009.*

De Clercq, H., Hayen , R., Cnudde, V., Boone, M. & Dusar, M. 2010a. The "Maagdentoren" of Zichem (Belgium): damage assessment of ferruginous sandstone by X-Ray Tomography. *8th International Symposium on the Conservation of Monuments of the Mediterranean Basin, Patras, 31 May–2 June 2010* Volume II, 206–219.

De Clercq, H., Hayen, R. & Dusar, M. 2010b. The "Maagdentoren" of Zichem (Belgium): damage assessment of ferruginous sandstone and strengthening effect of consolidation with ethylsilicate (TEOS). *8th International Symposium on the Conservation of Monuments of the Mediterranean Basin, Patras, 31 May–2 June 2010* Volume II, 20–235.

De Clercq, H. & Dusar, M. 2011. Materiaaltechnische studie van de buitenschil van een middeleeuws monument in ijzerzandsteen: de Maagdentoren in Zichem (in Dutch). *Handbook 'Onderhoud Renovatie Restauratie'*, Kluwer, V. 4, 1–28.

De Clercq, H., Hayen, R., Cnudde, V., Boone, M. & Dusar, M. 2012. Damage assessment of ferruginous sandstone by X-Ray tomography – The Virgin Tower of Zichem (Belgium). *12th International Congress on the Deterioration and Conservation of Stone Columbia University, New York, 22–26 Oct*.

De Schutter, G. & De Pauw, P. 2010. Research report for the Flemish Government, *Geotechniek*.

Deweerdt, T. 1980. Gallo-Romeinse villa te Bierbeek (in Dutch). *Hona*, 15/3, 39–41.

Deweerdt, T. & Provoost, A. 1982. Bierbeek: een Gallo-Romeinse villa (in Dutch). In: *Provoost A. (ed.), Het bodemarchief van Oost-Brabant. Le sous-sol archéologique du Brabant oriental*, Leuven, 19–21.

Doperé, F., Klinckaert, J., Minnen, B. & Van der Eycken, M. 2003. Brabantse bouwmeesters. Verhalen uit de late Middeleeuwen (in Dutch). *Bouwen met ijzerzandsteen in de Demerstreek, Provincie Vlaams Brabant*, Leuven.

Dreesen, R., De Ceukelaire, M. & De Koninck, R. 2010. Natuurlijk voorkomen en karakteristieken van inheemse natuursteen in Vlaanderen – Diestiaan ijzerzandsteen in het Hageland (in Dutch), *Study for ALBON (2010/SCT/R/006)*.

Dusar, M., Dreesen, R. & De Naeyer, A. 2009. Natuursteen in Vlaanderen (in Dutch). *Versteend verleden*, Mechelen: Kluwer.

Dusar, M., & De Ceukelaire, M., 2014. Voorkomen en ontginning van Diestiaan ijzerzandsteen, in: Diestiaan ijzerzandsteen, van Demergothiek tot restauratieproblematiek (in Dutch). *Study day 'Omgaan met Diestiaan ijzerzandsteengebruik', Diest, Begijnhof, 19th September 2014*, 19–26.

Hayen, R. & De Clercq, H. 2011. Material-technical research report on the development of a suitable repair mortar for facings in ferruginous sandstone of the Diest Formation (in Dutch).

Ingham J.P. 2008. Predicting the frost resistance of building stone. *Quarterly Journal of Engineering Geology and Hydrogeology*, 38, 387–399.

Middelbergpark 2009. De steen van Rotselaar (in Dutch) (http://www.middelberg.be/geschiedenis/desteen vanrotselaar.html)

Regionaal Landschap Noord-Hageland 2007. Groeves met een ijzersterk verhaal: De ijzerzandsteengroeves van het Hageland (in Dutch), *Regionaal Landschap Noord-Hageland*.

Triconsult, 2007. Sint-Eustachiuskerk te Zichem, Internal reports on the evaluation of the compressive strength and an endoscopic study of the masonry.

Van Campenhout, D. 2009. Verleden en toekomst van de exploitatie van ijzerzandsteen uit de Diestiaan als bouwsteen, een geologische studie (in Dutch), *Master thesis Earth and Environmental Sciences Departement,* K.U. Leuven.

Vandenberghe, N., Harris, W.B., Wampler, J.M., Houthuys, R., Louwye, S., Adriaens, R., Vos, K., Lanckacker, T., Matthijs, J., Deckers, J., Verhaegen, J., Laga, P., Westerhoff, W. & Munsterman, D. 2014. The implications of K-Ar glauconite dating of the Diest Formation on the paleogeography of the Upper Miocene in Belgium, *Geologica Belgica*, 17/2, 161–174.